

# Superhydrophobic/Superoleophilic MOF Composites for Oil–Water Separation

Ming-Liang Gao, Si-Yu Zhao, Zhi-Yan Chen, Lin Liu,\*<sup>1</sup> and Zheng-Bo Han\*<sup>2</sup>

College of Chemistry, Liaoning University, Shenyang 110036, P. R. China

## Supporting Information

**ABSTRACT:** A universal strategy is developed to construct metal-organic framework (MOF)-based superhydrophobic/superoleophilic materials by the reaction of activated MOFs and octadecylamine. In particular, S-MIL-101(Cr) composite can efficiently separate chloroform, toluene, petroleum ether, and *n*-hexane from water with excellent oil–water separation performance, with potential application in the environmental field.

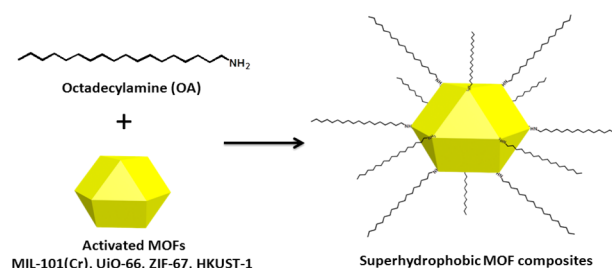
Industrial organic contaminants and oil spills have caused severe water pollution, which has led to a long-term threat to marine species and a disservice to human life.<sup>1</sup> Over the past decades, superhydrophobic materials applied in the oil-spill cleaning field have been developed to deal with oily wastewater.<sup>2</sup> To achieve superhydrophobicity, modifying the surface with low-surface-energy chemical composition or constructing a rough structure on a hydrophobic surface are two common methods.<sup>3</sup> However, a facile and universal strategy for preparing superhydrophobic materials that are used in the oil–water separation field is still an urgent task.

Emerging as a new class of porous materials, metal organic frameworks (MOFs) with high internal surface areas, unique adsorption properties, and rich functionalities have received increasing attention as potential adsorbent or separation materials.<sup>4</sup> From a biological point of view, major MOFs are degradable and harmless.<sup>5</sup> Therefore, MOFs that possess designed structure and tunable porosity are considered to be promising candidates to form novel superhydrophobic materials. In recent years, MOF-based superhydrophobic materials with high contact angles (CAs) have been fabricated.<sup>3c,6</sup> Currently, two main approaches are usually utilized to achieve MOF-based superhydrophobic materials.<sup>7</sup> On the one hand, the ligands containing aromatic hydrocarbon moieties are used to construct MOFs with highly corrugated anisotropic crystal morphologies. However, the syntheses of new superhydrophobic MOFs are unpredictable and demanding, which will restrict their practical applications. On the other hand, a long-chain or fluorinated polymer as molecular linker introduced to the pores or surface of MOFs is a conventional method to realize hydrophobicity.<sup>8</sup> Nonetheless, the tedious procedures and complicated additions would suppress the specific surface area of MOFs to further influence their properties. In addition, fluorinated materials are expensive, bioaccumulative and toxic for humans. Therefore, the accurate design and facile fabrication of superhydrophobic, environ-

ment-friendly MOF composites with high specific surface area is still a daunting challenge.

To address the above challenge, in this work, a universal strategy for preparing superhydrophobic MOF composites is presented. The reaction of the coordinative unsaturated metal sites of activated MOFs (MIL-101(Cr), UiO-66, ZIF-67, and HKUST-1) and octadecylamine (OA) was utilized to form superhydrophobic MOF composites (S-MOF). The long alkyl chain of OA with low surface energy was grafted onto the surface of MOFs, which would make MOFs have high water resistance and endow these composites with admirable superhydrophobicity; meanwhile, the inherent porosity of the MOFs would remain (Scheme 1). Owing to the above characteristic, the S-MOF composites exhibited excellent oil absorption capacity and oil/water selectivity, which offered a promising application prospect.<sup>9</sup>

## Scheme 1. Illustration Showing the Formation of Surface-Modified Superhydrophobic MOFs



S-MOF composites were performed by stirring the activated MOFs in a 10 mM OA toluene solution at 120 °C for 24 h. The unchanged powder X-ray diffraction (PXRD) patterns of S-MOF composites revealed that the OA modification occurs with no apparent loss of their crystallinity (Figure S1). The chemical stability of S-MOF composites was investigated by immersing them in different organic solvents (*n*-hexane, EtOH, MeOH, toluene, CH<sub>2</sub>Cl<sub>2</sub>, CHCl<sub>3</sub>, petroleum ether, ethyl acetate) and even in water for 24 h. The PXRD patterns verified that all of the crystalline structures of S-MOF composites are integrated (Figure S2). FT-IR spectra confirmed the presence of OA on the MOFs. As shown in Figure S3, compared with bare MOFs, the absorption bands of S-MOF composites were obviously enhanced at 2852 and 2924 cm<sup>-1</sup>, which corresponded to the stretching vibration of

Received: November 26, 2018

C–H in methylene of OA.<sup>10</sup> The chemical stability of S-MOF composites was further confirmed by FT-IR spectra after immersion in different solvents. The results showed that the bands of  $-\text{CH}_2-$  groups still existed. In addition, the IR spectra at  $745$  and  $713\text{ cm}^{-1}$  can be attributed to the formation of the N–Cr band, and X-ray photoelectron spectroscopy (XPS) can also directly verify the coordination of the amino group of OA to the  $\text{Cr}^{3+}$  centers (Figures S4 and S5). The EDS element mapping was investigated by the S-MIL-101(Cr) composite. As shown in Figure 1a, the presence of a N element

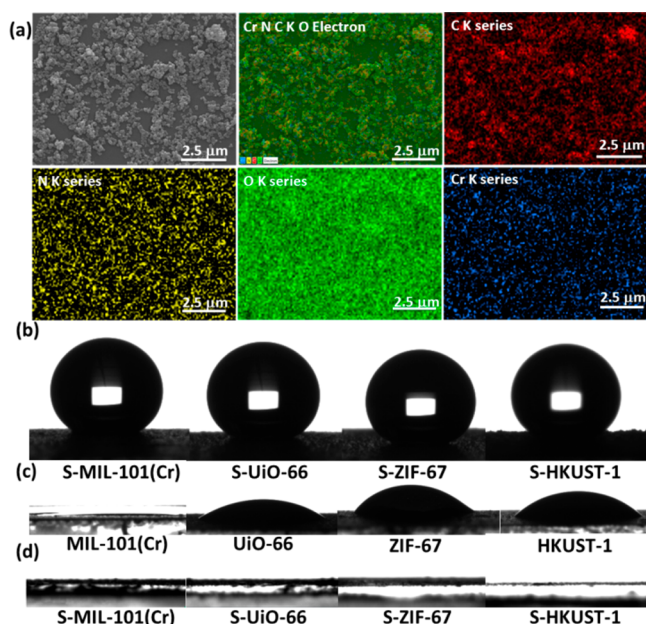


**Figure 1.** (a) SEM images and the corresponding elemental mapping of S-MIL-101(Cr). (b) Water CAs of S-MOFs (S-MIL-101(Cr), S-UiO-66, S-ZIF-67, and S-HKUST-1). (c) Water CAs of MOFs (S-MIL-101(Cr), S-UiO-66, S-ZIF-67, and S-HKUST-1). (d) Oil CAs of S-MOFs (S-MIL-101(Cr), S-UiO-66, S-ZIF-67, and S-HKUST-1).

in the OA molecule was observed, which also confirms that the S-MOF-101(Cr) composite is successfully prepared. The SEM images of S-MIL-101(Cr) composite compared with bare MIL-101(Cr) confirmed the intact morphologies and no obvious change in size (Figure S6a,b). In addition, the surface of the S-MIL-101(Cr) composite was smooth, and there was no significant change, which was possibly due to a small quantity of OA molecule existing in S-MIL-101(Cr) composite that cannot be observed via SEM. The same phenomena were also observed in the other three composites (Figure S6). The resulting surface modification is visible in the nitrogen adsorption–desorption isotherms of the S-MOF composites.<sup>11</sup> The adsorption and desorption isotherms of the four MOFs before and after OA-grafting are shown in Figure S7. The BET surface areas are  $2546$  ( $2438$ ),  $1248$  ( $1146$ ),  $1825$  ( $1775$ ), and  $1750$  ( $1727$ )  $\text{m}^2\cdot\text{g}^{-1}$  for MIL-101(Cr) (S-MIL-101(Cr)), UiO-66 (S-UiO-66), ZIF-67 (S-ZIF-67), and HKUST-1 (S-HKUST-1), respectively. Nonlocal density functional theory (NLDFT) method was utilized to analyze the pore-size distribution of the MOFs and S-MOF composites (Figure S8) and demonstrated little difference after modification of the surface of MOFs. The results show that the bare MOFs and the OA-grafted MOFs have nearly the same BET

surface areas and pore-size distribution, which implied that the OA molecules may exist on the surface of MOFs.

Static water CA measurements were performed to evaluate the surface wettability of S-MOF composites (Figure 1b,c). The CA of a water droplet ( $10\ \mu\text{L}$ ) on bare MIL-101(Cr) was estimated to be  $\sim 2^\circ$  (Figure 1b). It is interesting that the water CA of S-MIL-101(Cr) composite can reach  $\sim 156^\circ$  after OA modification. This superhydrophobic property is primarily ascribed to the inherent hydrophobic chain of OA on the surface of S-MIL-101(Cr).<sup>12</sup> After grafted with OA molecules, the surface character of the MIL-101(Cr) can easily transform from hydrophilic to hydrophobic. The CA of a water droplet of S-UiO-66, S-ZIF-67, and S-HKUST-1 samples is similar to that of S-MIL-101(Cr), and all showed  $>150^\circ$ . Interestingly, an oil droplet rapidly penetrates into the S-MOF composites in  $<10\text{ s}$ , and the oil CAs were measured to be  $0^\circ$ , implying the superoleophilic nature (Figure 1d). As shown in Figure S9, a droplet of dyestuff dyed water or  $\text{CHCl}_3$  was dropped on the S-MOF composites after grafted with the OA molecule. These images can also display the superhydrophobic and superoleophilic properties of the S-MOF composites. In contrast, the S-MIL-101(Cr) composite demonstrates a competitive water CA value ( $\sim 156^\circ$ ) compared with the reported MOF-based hydrophobic materials, MOFF-2 ( $151 \pm 1^\circ$ ), SH ZIF-67 ( $146^\circ$ ),  $\text{Cu}_3(\text{NH-AM}_{10}\text{-BTC})_2$  ( $147^\circ$ ), OPA-UiO-66 ( $160^\circ$ ), ZIF-7-300 ( $154.7^\circ$ ), ZIF-90 ( $152.4^\circ$ ), and UH-MOF-100 ( $176^\circ$ ) (Table S1).<sup>6b–g,8b</sup> All of the above results supported the fact that S-MOF composites may exhibit a promising potential application in removing toxic organic contaminants in the environmental field.

On the basis of the excellent porosity and surface wettability, S-MOF composites should be admirable candidates for the absorption of organic solvents. The absorption capacity of S-MOF composites toward various organic solvents (especially nonpolar or weakly polar organic solvents) was explored by using a procedure similar to that reported by Li and coworkers.<sup>13</sup> In a typical absorption measurement, toluene was added to the postsynthetic grafted S-MOF powder at room temperature and then kept for 30 min to achieve saturated absorption; then, the samples were separated by centrifugation and finally weighed. The adsorption efficiencies of these S-MOF composites for organic phase were calculated according to equation:  $Q = (W_{\text{saturated absorption}} - W_{\text{initial}})/W_{\text{initial}} \times 100\%$ . The adsorption capacities of *n*-hexane, EtOH, MeOH,  $\text{CH}_2\text{Cl}_2$ ,  $\text{CHCl}_3$ , petroleum ether, and ethyl acetate were also tested. As shown in Figure S10, the bare MOFs and S-MOF composites both showed high absorption capacities for the organic phase. The bare MOFs showed the absorption capacities in the range of  $118$ – $281\text{ wt } \%$  (MIL-101(Cr)),  $81$ – $219\text{ wt } \%$  (HKUST-1),  $75$ – $193\text{ wt } \%$  (UiO-66), and  $86$ – $231\text{ wt } \%$  (ZIF-67). In contrast the adsorption capacities of S-MOFs were enhanced and ranged between  $142$  and  $369\text{ wt } \%$  (S-MIL-101(Cr)),  $118$  and  $325\text{ wt } \%$  (S-HKUST-1),  $125$  and  $281\text{ wt } \%$  (S-UiO-66), and  $122$  and  $341\text{ wt } \%$  (S-ZIF-67). These results indicated that the hydrophobic nature of S-MOF composites was crucial for the high adsorption capacities.

Because of the superhydrophobic and superoleophilic properties of S-MOF composites, the practical oil–water separation performance could be investigated. Bearing this approach in mind, the separation device was generated by loading S-MIL-101(Cr) composite on commercial filter paper according to the previous reports.<sup>13b,14</sup> Heavy oil can be separated from the oil–water mixture under the force of

gravity without any external force. In brief,  $\text{CHCl}_3$  as a characteristic heavy oil was selected as a model, and the oil–water mixture was generated by mixing  $\text{CHCl}_3$  and dyed water to test the separation performance. The separation equipment images before and after the separation experiment were demonstrated in Figure S11. In the process of separation,  $\text{CHCl}_3$  easily permeated through the filter paper, which was fixed between two glass devices, but the water was repelled and stayed in upper part of the glass container, and the collected efficiency of  $\text{CHCl}_3$  was  $\sim 99.9\%$ . This phenomenon revealed that the S-MIL-101(Cr) composite coating can effectively separate oil–water mixtures. As shown in Figure 2a, the

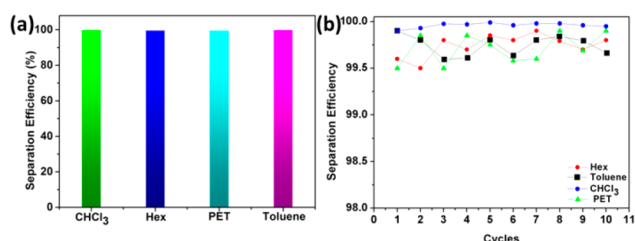


**Figure 2.** (a) Separation efficiency of different organic solvents by S-MIL-101(Cr) composite. (b) Recycled experiment for separating different oils from water by S-MIL-101(Cr) composite.

separation performances of the S-MIL-101(Cr) composite for light oils (for example, toluene, Hex, and PET) were also investigated, and the separation efficiencies were all  $>99.5\%$ . The oil–water mixture separation mechanism can be attributed to OA molecules on the surface of S-MIL-101(Cr) composite endowing MIL-101(Cr) with superhydrophobic properties. Oil can be allowed to pass through the S-MIL-101(Cr) composite coating, and water is prevented on the coating. Furthermore, the S-MIL-101(Cr) composite coating showed excellent recycling performance even after being recycled 10 cycles, and the separation performance was nearly unchanged (Figure 2b). The PXRD and FT-IR spectra revealed that the structural integrity of S-MIL-101(Cr) composite remained well even after 10 cycles, indicating its great recyclability and excellent stability for oil–water separation (Figure S12). Compared with the previous reported superhydrophobic materials, S-MIL-101(Cr) composite revealed competitive oil–water separation efficiency and recyclability (Table S2). All of these results make unique S-MIL-101(Cr) composite a promising oil–water separation material for practical applications.

In conclusion, a universal strategy of constructing superhydrophobic and superoleophilic MOF composites has been developed by the reaction of activated MOFs and octadecylamine. The porosity and crystallinity of the as-synthesized MOF materials are nearly unchanged by this strategy. All four S-MOF composites exhibited surface superhydrophobicity with water CA  $>150^\circ$ , which should contribute to the strongly hydrophobic chemical compositions. They all demonstrated high adsorption capacities toward organic solvents and exhibited excellent oil–water separation performance ( $>99.5\%$ ) without external pressure. We envision that this strategy will open an avenue for improving the water stability and superhydrophobic performance of MOFs.

## ■ ASSOCIATED CONTENT

### 📄 Supporting Information

The Supporting Information is available free of charge on the ACS Publications website at DOI: 10.1021/acs.inorgchem.8b03293.

Materials and general methods, PXRD, FT-IR, XPS, nitrogen adsorption–desorption isotherms, and SEM images (PDF)

## ■ AUTHOR INFORMATION

### Corresponding Authors

\*Z.-B.H.: E-mail: ceshzb@lnu.edu.cn.

\*L.L.: E-mail: liulin@lnu.edu.cn.

### ORCID

Lin Liu: 0000-0002-9164-1190

Zheng-Bo Han: 0000-0001-8635-9783

### Notes

The authors declare no competing financial interest.

## ■ ACKNOWLEDGMENTS

We thank the National Natural Science Foundation of China for their financial support (21671090 and 21701076) and Liaoning Province Doctor Startup Fund (20180540056).

## ■ REFERENCES

- (1) (a) Chu, Z.; Belding, L.; van der Est, A.; Dudding, T.; Korobkov, I.; Nikonov, G. I. A Coordination Compound of Ge0 Stabilized by a Diiminopyridine Ligand. *Angew. Chem., Int. Ed.* **2014**, *53*, 2711–2715. (b) Jin, M. H.; Wang, J.; Yao, X.; Liao, M.; Zhao, Y.; Jiang, L. Underwater Oil Capture by a Three-Dimensional Network Architected Organosilane Surface. *Adv. Mater.* **2011**, *23*, 2861–2864.
- (2) (a) Zhang, W.; Shi, Z.; Zhang, F.; Liu, X.; Jin, J.; Jiang, L. Superhydrophobic and superoleophilic PVDF membranes for effective separation of water-in-oil emulsions with high flux. *Adv. Mater.* **2013**, *25*, 2071–2076. (b) Darmanin, T.; Guittard, F. Recent advances in the potential applications of bioinspired superhydrophobic materials. *J. Mater. Chem. A* **2014**, *2*, 16319–16359. (c) Xiao, Z.; Zhang, M.; Fan, W.; Qian, Y.; Yang, Z.; Xu, B.; Kang, Z.; Wang, R.; Sun, D. Highly efficient oil/water separation and trace organic contaminants removal based on superhydrophobic conjugated microporous polymer coated devices. *Chem. Eng. J.* **2017**, *326*, 640–646.
- (3) (a) Wang, B.; Liang, W.; Guo, Z.; Liu, W. Biomimetic superhydrophobic and superoleophilic materials applied for oil/water separation: a new strategy beyond nature. *Chem. Soc. Rev.* **2015**, *44*, 336–361. (b) Rao, K. P.; Higuchi, M.; Sumida, K.; Furukawa, S.; Duan, J.; Kitagawa, S. Design of superhydrophobic porous coordination polymers through the introduction of external surface corrugation by the use of an aromatic hydrocarbon building unit. *Angew. Chem., Int. Ed.* **2014**, *53*, 8225–8230. (c) Jayaramulu, K.; Datta, K. K. R.; Rösler, C.; Petr, M.; Otyepka, M.; Zboril, R.; Fischer, R. A. Biomimetic Superhydrophobic/Superoleophilic Highly Fluorinated Graphene Oxide and ZIF-8 Composites for Oil-Water Separation. *Angew. Chem., Int. Ed.* **2016**, *55*, 1178–1182. (d) Gao, X.; Zhou, J.; Du, R.; Xie, Z.; Deng, S.; Liu, R.; Liu, Z.; Zhang, J. Robust superhydrophobic foam: a graphdiyne-based hierarchical architecture for oil/water separation. *Adv. Mater.* **2016**, *28*, 168–173.
- (4) (a) Furukawa, H.; Cordova, K. E.; O’Keeffe, M.; Yaghi, O. M. The chemistry and applications of metal-organic frameworks. *Science* **2013**, *341*, 1230444. (b) Li, J. R.; Kuppler, R. J.; Zhou, H. C. Selective gas adsorption and separation in metal-organic frameworks. *Chem. Soc. Rev.* **2009**, *38*, 1477–1504. (c) Kitao, T.; Zhang, Y.; Kitagawa, S.; Wang, B.; Uemura, T. Hybridization of MOFs and polymers. *Chem. Soc. Rev.* **2017**, *46*, 3108–3133. (d) Sun, Q.; Aguila, B.; Perman, J. A.; Butts, T.; Xiao, F. S.; Ma, S. Q. Integrating Superwettability within



Covalent Organic Frameworks for Functional Coating. *Chem.* **2018**, *4*, 1726–1739. (e) Chen, Y.; Li, S.; Pei, X.; Zhou, J.; Feng, X.; Zhang, S.; Cheng, Y.; Li, H.; Han, R.; Wang, B. A Solvent-Free Hot-Pressing Method for Preparing Metal-Organic-Framework Coatings. *Angew. Chem., Int. Ed.* **2016**, *55*, 3419–3423. (f) Wei, N.; Zhang, Y.; Liu, L.; Han, Z. B.; Yuan, D. Q. Pentanuclear Yb(III) cluster-based metal-organic frameworks as heterogeneous catalysts for CO<sub>2</sub> conversion. *Appl. Catal., B* **2017**, *219*, 603–610. (g) Gao, M. L.; Wang, W. J.; Liu, L.; Han, Z. B.; Wei, N.; Cao, X. M.; Yuan, D. Q. Microporous Hexanuclear Ln(III) Cluster-Based Metal-Organic Frameworks: Color Tunability for Barcode Application and Selective Removal of Methylene Blue. *Inorg. Chem.* **2017**, *56*, 511–517.

(5) Horcajada, P.; Gref, R.; Baati, T.; Allan, P. K.; Maurin, G.; Couvreur, P.; Férey, G.; Morris, R. E.; Serre, C. Metal-organic frameworks in biomedicine. *Chem. Rev.* **2012**, *112*, 1232–1268.

(6) (a) Xie, L. H.; Liu, X. M.; He, T.; Li, J. R. Metal-Organic Frameworks for the Capture of Trace Aromatic Volatile Organic Compounds. *Chem.* **2018**, *4*, 1911–1927. (b) Chen, T.; Popov, I.; Zenasni, O.; Daugulis, O.; Miljanic, O. S. Superhydrophobic perfluorinated metal-organic frameworks. *Chem. Commun.* **2013**, *49*, 6846–6848. (c) Qian, X.; Sun, F.; Sun, J.; Wu, H.; Xiao, F.; Wu, X.; Zhu, G. Imparting surface hydrophobicity to metal-organic frameworks using a facile solution-immersion process to enhance water stability for CO<sub>2</sub> capture. *Nanoscale* **2017**, *9*, 2003–2008. (d) Rubin, H. N.; Reynolds, M. M. Functionalization of metal-organic frameworks to achieve controllable wettability. *Inorg. Chem.* **2017**, *56*, 5266–5274. (e) Sun, Y.; Sun, Q.; Huang, H.; Aguila, B.; Niu, Z.; Perman, J. A.; Ma, S. Q. A molecular-level superhydrophobic external surface to improve the stability of metal-organic frameworks. *J. Mater. Chem. A* **2017**, *5*, 18770–18776. (f) Zhang, G.; Zhang, J.; Su, P.; Xu, Z.; Li, W.; Shen, C.; Meng, Q. Non-activation MOF arrays as a coating layer to fabricate a stable superhydrophobic micro/nano flower-like architecture. *Chem. Commun.* **2017**, *53*, 8340–8343. (g) Liu, C.; Liu, Q.; Huang, A. A superhydrophobic zeolitic imidazolate framework (ZIF-90) with high steam stability for efficient recovery of bioalcohols. *Chem. Commun.* **2016**, *52*, 3400–3402. (h) Wang, S.; Morris, W.; Liu, Y.; McGuirk, C. M.; Zhou, Y.; Hupp, J. T.; Farha, O. K.; Mirkin, C. A. Surface-Specific Functionalization of Nanoscale Metal-Organic Frameworks. *Angew. Chem., Int. Ed.* **2015**, *54*, 14738–14742.

(7) (a) Serre, C. Superhydrophobicity in highly fluorinated porous metal-organic frameworks. *Angew. Chem., Int. Ed.* **2012**, *51*, 6048–6050. (b) Nguyen, J. G.; Cohen, S. M. Moisture-resistant and superhydrophobic metal-organic frameworks obtained via postsynthetic modification. *J. Am. Chem. Soc.* **2010**, *132*, 4560–4561. (c) Zhou, H. C.; Kitagawa, S. Metal-organic frameworks (MOFs). *Chem. Soc. Rev.* **2014**, *43*, 5415–5418. (d) Dong, X.; Chen, J.; Ma, Y.; Wang, J.; Chan-Park, M. B.; Liu, X.; Wang, L.; Huang, W.; Chen, P. Superhydrophobic and superoleophilic hybrid foam of graphene and carbon nanotube for selective removal of oils or organic solvents from the surface of water. *Chem. Commun.* **2012**, *48*, 10660–10662.

(8) (a) Yang, C.; Kaipa, U.; Mather, Q. Z.; Wang, X.; Nesterov, V.; Venero, A. F.; Omary, M. A. Fluorous metal-organic frameworks with superior adsorption and hydrophobic properties toward oil spill cleanup and hydrocarbon storage. *J. Am. Chem. Soc.* **2011**, *133*, 18094–18097. (b) Mukherjee, S.; Kansara, A. M.; Saha, D.; Gonnade, R.; Mullangi, D.; Manna, B.; Desai, A. V.; Thorat, S. H.; Singh, P. S.; Mukherjee, A.; Ghosh, S. K. An ultrahydrophobic fluorous metal-organic framework derived recyclable composite as a promising platform to tackle marine oil spills. *Chem. - Eur. J.* **2016**, *22*, 10937–10943. (c) Roy, S.; Suresh, V. M.; Maji, T. K. Self-cleaning MOF: realization of extreme water repellence in coordination driven self-assembled nanostructures. *Chem. Sci.* **2016**, *7*, 2251–2256.

(9) (a) Guerrero, G.; Mutin, P. H.; Vioux, A. Anchoring of phosphonate and phosphinate coupling molecules on titania particles. *Chem. Mater.* **2001**, *13*, 4367–4373. (b) Boissezon, R.; Muller, J.; Beaugeard, V.; Monge, S.; Robin, J. J. Organophosphonates as anchoring agents onto metal oxide-based materials: synthesis and applications. *RSC Adv.* **2014**, *4*, 35690–35707.

(10) (a) Abánades Lázaro, I. A.; Haddad, S.; Sacca, S.; Orellana-Tavra, C.; Fairen-Jimenez, D.; Forgan, R. S. Selective Surface PEGylation of UiO-66 Nanoparticles for Enhanced Stability, Cell Uptake, and pH-Responsive Drug Delivery. *Chem.* **2017**, *2*, 561–578. (b) Guo, X.; Liu, D.; Han, T.; Huang, H.; Yang, Q.; Zhong, C. Preparation of thin film nanocomposite membranes with surface modified MOF for high flux organic solvent nanofiltration. *AIChE J.* **2017**, *63*, 1303–1312.

(11) (a) Peng, Y.; Zhao, M.; Chen, B.; Zhang, Z.; Huang, Y.; Dai, F.; Lai, Z.; Cui, X.; Tan, C.; Zhang, H. Hybridization of MOFs and COFs: A New Strategy for Construction of MOF@COF Core-Shell Hybrid Materials. *Adv. Mater.* **2018**, *30*, 1705454. (b) Liu, L.; Wang, S. M.; Han, Z. B.; Ding, M.; Yuan, D. Q.; Jiang, H. L. Exceptionally Robust In-Based Metal-Organic Framework for Highly Efficient Carbon Dioxide Capture and Conversion. *Inorg. Chem.* **2016**, *55* (7), 3558–3565. (c) Zhang, Y.; Wang, Y.; Liu, L.; Wei, N.; Gao, M. L.; Zhao, D.; Han, Z. B. Robust Bifunctional Lanthanide Cluster Based Metal-Organic Frameworks (MOFs) for Tandem Deacetalization-Knoevenagel Reaction. *Inorg. Chem.* **2018**, *57* (4), 2193–2198.

(12) Zhang, M.; Xin, X.; Xiao, Z.; Wang, R.; Zhang, L.; Sun, D. A multi-aromatic hydrocarbon unit induced hydrophobic metal-organic framework for efficient C<sub>2</sub>/C<sub>1</sub> hydrocarbon and oil/water separation. *J. Mater. Chem. A* **2017**, *5*, 1168–1175.

(13) (a) Li, A.; Sun, H. X.; Tan, D. Z.; Fan, W. J.; Wen, S. H.; Qing, X. J.; Li, G. X.; Li, S. Y.; Deng, W. Q. Superhydrophobic conjugated microporous polymers for separation and adsorption. *Energy Environ. Sci.* **2011**, *4*, 2062–2065. (b) Shi, Q.; Sun, H.; Yang, R.; Zhu, Z.; Liang, W.; Tan, D.; Yang, B.; Li, A.; Deng, W. Synthesis of conjugated microporous polymers for gas storage and selective adsorption. *J. Mater. Sci.* **2015**, *50*, 6388–6394. (c) Mu, P.; Sun, H.; Zang, J.; Zhu, Z.; Liang, W.; Yu, F.; Chen, L.; Li, A. Facile tuning the morphology and porosity of a superwetting conjugated microporous polymers. *React. Funct. Polym.* **2016**, *106*, 105–111.

(14) Mullangi, D.; Shalini, S.; Nandi, S.; Choksi, B.; Vaidhyanathan, R. Super-hydrophobic covalent organic frameworks for chemical resistant coatings and hydrophobic paper and textile composites. *J. Mater. Chem. A* **2017**, *5*, 8376–8384.